JOURNAL OF NANO- AND ELECTRONIC PHYSICS
Vol. **10** No 5, 05036(5pp) (2018)

ЖУРНАЛ НАНО- ТА ЕЛЕКТРОННОЇ ФІЗИКИ
Том **10** № 5, 05036(5cc) (2018)

The Electronic Band Structure of the $BaSnO_3$ and $SrSnO_3$ Perovskites Calculated within the GGA and GW Approaches

S.V. Syrotyuk*, I.Ye. Lopatynskyi, V.M. Shved

Lviv Polytechnic National University, 12, S. Bandera Str., 79013 Lviv, Ukraine

(Received 08 July 2018; revised manuscript received 22 October 2018; published online 29 October 2018)

The Green's function method, implemented in the first order of the perturbation theory (GW), was applied for an accurate description of the electronic structure of cubic $BaSnO_3$ and $SrSnO_3$ perovskites. First, the band structure of these materials was calculated within the generalized gradient approximation (GGA). Then, in order to obtain the accurate band gaps, the quasiparticle corrections to the eigenenergies were evaluated. The calculated electronic structure by means of the GW approximation was compared to the structure obtained within the GGA. The application of quasiparticle corrections to the eigenenergies led to a significant widening of the band gaps and provided a much better agreement with the experimental data. The GW corrections to the band energies, found for both crystals at the points of the first Brillouin zone, are quite different. Consequently, the use of a scissor operator can lead to errors in a calculation of the optical constants.

Keywords: Perovskites, Electronic structure, Green's function, GW, Quasiparticles.

DOI: 10.21272/jnep.10(5).05036 PACS numbers: 71.15.Mb, 71.20.Nr, 71.35. ±

1. INTRODUCTION

$(Ba,Sr)SnO_3$ perovskites have been under intensive investigation due to their attractive properties such as high electron mobility at room temperature and optical transparency in visible region. Wide-band gap $(Ba,Sr)SnO_3$ compounds can be used in solar photovoltaics, displays and transparent conductor applications [1, 2]. These perovskites were also investigated for technological applications in lithium-ion batteries [3]. Recently, $BaSnO_3$ has been proposed to be a gas sensor material due to its good sensitivity to SO_2 [4]. In addition $(Ba,Sr)SnO_3$ perovskites are potential photocatalysts for water splitting [5, 6].

In the bulk La-doped $BaSnO_3$ single crystals the electron mobility of 320 $cm^2/V{\cdot}s$ was achieved [7]. While the carrier mobility in La-doped $SrSnO_3$ was reported to be 40 $cm^2/V{\cdot}s$ [8]. For example, in popular $SrTiO_3$ much lower values of the electron mobility (5-11 $cm^2/V{\cdot}s$) have been observed [9]. The possibility to increase the carrier mobility in $BaSnO_3$ has been investigated systematically by controlling defects and using heterostructure engineering [10-12]. In order to understand the reasons for the high electron mobility, it is important to know the electronic structure of $(Ba,Sr)SnO_3$.

$BaSnO_3$ is the cubic perovskite with indirect band gap of 3.1-3.4 eV [13, 14]. In general, $SrSnO_3$ exists in the cubic and orthorhombic types of structure and has more wide indirect gap ranging between 4.1 and 4.27 eV [13, 15]. Electronic structure calculations of $(Ba,Sr)SnO_3$ crystals have been performed within different approximations for the exchange-correlation functional [16-19, 35, 37]. But existing calculations obtained in the general gradient approximation (GGA) significantly underestimate band gaps [16, 17, 35]. Applying hybrid functional or TB-mBJ potential could improve accuracy of the calculations and the higher energy band gaps have been obtained in $(Ba, Sr)SnO_3$ [16, 18, 19, 37]. But proper description of their electronic structure is still an area of research.

Recently, the DFT-ACBN0 [38] method was successfully applied to the band structure calculations of $BaSnO_3$ and obtained gap value is in a good agreement with the experimental results [20]. An alternative approach is so-called GW approximation [21] based on the many-body perturbation theory and it is an accurate way to predict the fundamental gaps and band structure of solids. The main focus is on taking screening into account in combination with the Green's function theory. The band gap dependence of $BaSnO_3$ on a strain has already been studied within the GW approach [22]. But GW calculations of the electronic structure of $(Ba,Sr)SnO_3$ perovskites are still absent.

In this work, as a first step the electron energy spectrum and the wave functions of $(Ba,Sr)SnO_3$ have been calculated by means of the GGA. Then quasiparticle corrections to the eigenenergies were obtained taking into account the Coulomb exchange interaction and the Green's functions calculated in terms of the GGA results. Consequently, the GW method was used. The quasiparticle-like electronic structures of $(Ba,Sr)SnO_3$ perovskites are obtained for the first time.

2. CALCULATION

We will seek the quasiparticle energies as the poles of the Green's function. The basic functions, necessary for constructing the latter, are obtained from the Kohn-Sham equation [24]:

$$(-\Delta^2 + V_{ext}(\boldsymbol{r}) + V_H(\boldsymbol{r}) + V_{xc}(\boldsymbol{r}))\varphi_{n\boldsymbol{k}}(\boldsymbol{r}) = \varepsilon_{n\boldsymbol{k}}\varphi_{n\boldsymbol{k}}(\boldsymbol{r}), \quad (1)$$

where $-\nabla^2$ is the kinetic energy operator, and V_{ext} denotes the ionic pseudopotential, and V_H , V_{XC} are the Hartree and exchange-correlation potential, respectively. The wave vector in the Brillouin zone is represented by $\boldsymbol{k}$ and n is the band index. The quasiparticle ener-

* svsnpe@gmail.com

gies and eigenfunctions are determined from the quasiparticle equation [25, 26]:

$$\begin{aligned}&(-\nabla^2 + V_{ext}(\mathbf{r}) + V_H(\mathbf{r}))\psi_{n\mathbf{k}}(\mathbf{r}) \\ &+\int \Sigma(\mathbf{r},\mathbf{r}', E_{n\mathbf{k}})\psi_{n\mathbf{k}}(\mathbf{r}')d\mathbf{r}' = E_{n\mathbf{k}}\psi_{n\mathbf{k}}(\mathbf{r})\end{aligned}, \quad (2)$$

where Σ is the non-local self-energy operator. The wave functions are searched on basis of the single-particle states obtained from Eq. (1):

$$\psi_{n\mathbf{k}}(\mathbf{r}) = \sum_{n'} a_{nn'}\varphi_{n'\mathbf{k}}(\mathbf{r}) . \quad (3)$$

From Eqs. (1) – (3) the perturbative quasiparticle Hamiltonian is obtained in the form

$$H_{nn'}(E) = \varepsilon_{n\mathbf{k}}\delta_{nn'} + < \varphi_{n\mathbf{k}} \mid \Sigma(E) - V_{xc} \mid \varphi_{n'\mathbf{k}} > , \quad (4)$$

where the second term in Eq. (4) represents a perturbation.

All calculations were performed using the ABINIT software package [27]. Integration over the Brillouin zone was carried out on $8 \times 8 \times 8$ Monkhorst-Pack [28] grid in the reciprocal space. The projector augmented wave datasets were used for Ba, Sr, Sn and O atoms [29]. The valence basis states were $5s^2 5p^6 6s^2 5d^0$ for Ba, $4s^2 4p^6 5s^2 4d^0$ for Sr, $4d^{10} 5s^2\ 5p^2$ for Sn, $2s^2 2p^4$ for O with the radii of the augmentation spheres of 2.31, 2.21, 2.38, 1.41 a.u., respectively. The energy cutoff of 870 eV was used for the wave function expansion. The contour deformation method proposed by S. Faleev et al. was chosen for GW electronic structure calculations [30].

The Broyden–Fletcher–Goldfarb–Shanno [31] minimization of the total energy was used for the structural relaxation of (Ba,Sr)SnO_3 after which stresses below 0.003 GPa were obtained. In $BaSnO_3$ the lattice constant of 4.180 Å was found after the relaxation which is higher by 1.7% then the experimental data of 4.108 Å [32]. In work [33] almost the same lattice constant of $BaSnO_3$ was obtained after the geometry optimization. In $SrSnO_3$ crystal the calculated lattice constant of 4.103 Å is in a good agreement with the experimental value of 4.025 Å [32]. The symmetry of the cubic perovskites (Ba,Sr)SnO_3 is described by Pm-3m space group, and the Brave lattices are primitive cubic.

3. RESULTS AND DISCUSSION

The band structure of $BaSnO_3$ crystal, calculated within the GGA and GW approximations are present in Fig. 1 and Fig. 2, respectively. The valence band maximum is chosen for a zero of energy. In both figures the bottom of the conduction band is at Γ point and the top of the valence band occurs at R point. The indirect band gap of 0.4 eV is found by means of the GGA in $BaSnO_3$, whereas the GW method yields the energy band gap of 3.29 eV (the experimental values are in a range 3.1–3.4 eV). The conduction band of $BaSnO_3$ crystal is characterized by a large dispersion of the curves and that can affect on the carrier mobility. In Fig. 2 the top of the valence band at M point is lower by 0.09 eV then the valence band maximum at R point. After detailed comparison of Fig. 1 and Fig. 2 we can see clearly the differences in localization of the valence band energy levels obtained by different approximations. The energy levels located nearly at – 20 eV (Fig. 1) are formed mainly from hybridized Ba *d* and Sn *d* states as shown in Fig. 3. Figure 3 represent the total and partial densities of states of $BaSnO_3$ calculated within the GGA method. Also at Γ point the energy levels of $BaSnO_3$ localized at – 10.29 eV (Fig. 1) occur lower by 0.75 eV in Fig. 2. These levels are formed by Ba *s*, *p*, *d* states and O *s* orbitals**.** The top of the valence band consists of hybridized Ba *p* and O *p* states as well as Sn *p* states. The bottom of the conduction band is formed by Ba *p*, Sn *s, p* and O *s, p* orbitals.

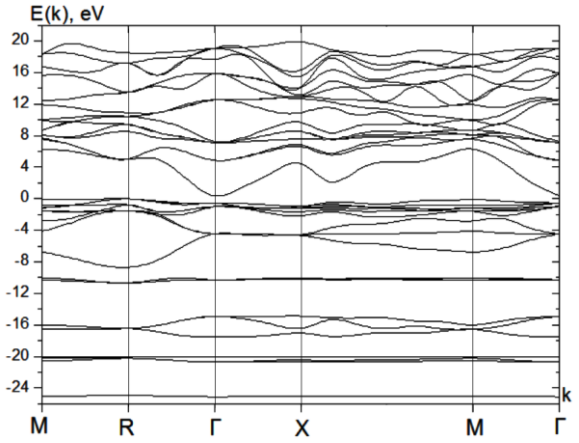

Fig. 1 – The electronic structure of $BaSnO_3$ obtained within the GGA

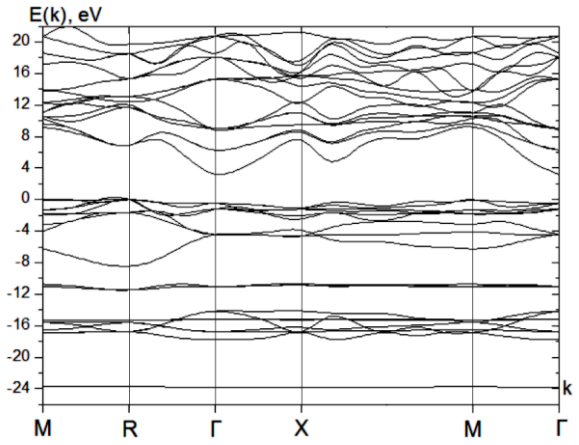

Fig. 2 – The electronic structure of $BaSnO_3$ obtained within the GW approximation

The energy levels in the upper part of the valence band, obtained within the GGA and GW approaches, are located in the energy intervals from -8.0 to 0.0 eV, respectively. In contrast, the energy of the electrons in the conduction band, obtained in these two approaches, are very different. The band gaps of $BaSnO_3$ at the high symmetry points calculated in both approximations (E_{GW} and E_{GGA}) are presented in Table 1. As can be seen, the differences between the values of band gaps, obtained within the GW and GGA (E_{GW}-E_{GGA}), are very significant.

The calculated band structure of cubic $SrSnO_3$ within the GGA and GW approaches are shown in Fig. 5 and Fig. 6, respectively. The indirect Γ-R gap, obtained in the GGA, equals 1.04 eV and is well compared with other theoretical findings [17, 35].

Table 1 – The calculated direct and indirect band gaps of (Ba,Sr)SnO_3 crystals

$BaSnO_3$			
	E_{GGA}	E_{GW}	$E_{GW}-E_{GGA}$
Γ-R	0.396	3.289	2.893
Γ-Γ	0.920	3.756	2.836
X-X	5.403	8.654	3.251
M-M	6.374	9.355	2.981
R-R	5.031	6.958	1.928
$SrSnO_3$			
	E_{GGA}	E_{GW}	$E_{GW}-E_{GGA}$
Γ-R	1.041	4.279	3.238
Γ-Γ	1.862	5.112	3.250
X-X	6.186	9.809	3.623
M-M	6.844	9.967	3.123
R-R	5.421	7.796	2.375

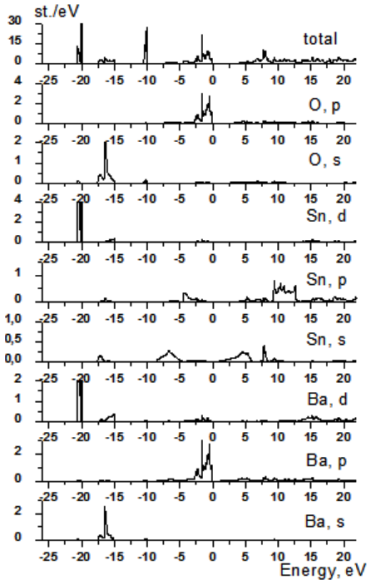

Fig. 3 – The partial and total densities of states of $BaSnO_3$ obtained within the GGA

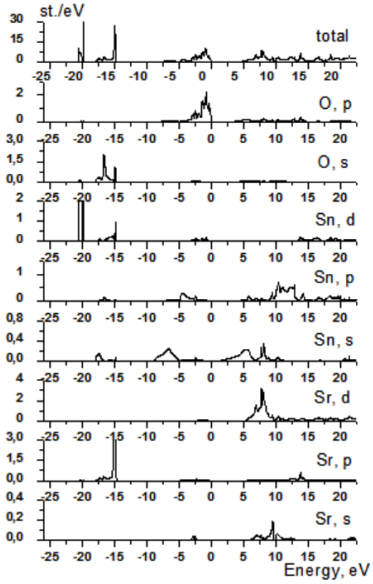

Fig. 4 – The partial and total densities of states of $SrSnO_3$ obtained within the GGA

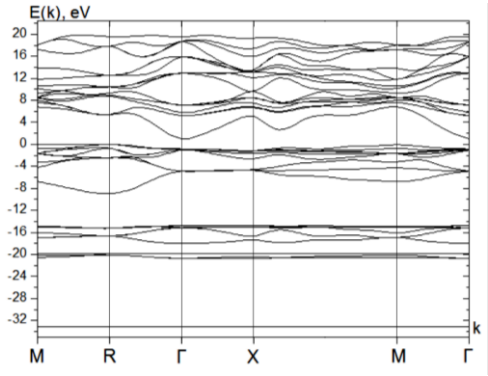

Fig. 5 – The electronic structure of $SrSnO_3$ obtained within the GGA

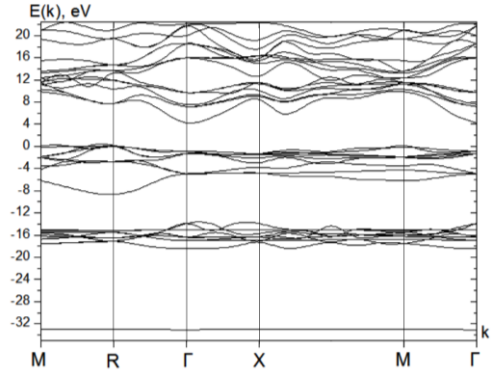

Fig. 6 – The electronic structure of $SrSnO_3$ obtained within the GW approximation

The GW band gap of crystal $SrSnO_3$ equals 4.28 eV and is well compared to the measured results (the experimental values are in a range 4.1-4.27 eV). The upper part of the valence band in a crystal $SrSnO_3$ is formed by Sn *p* and O *p* states, and the bottom of the conduction band mainly consists of Sr *s, d*, Sn *s, p* and O *p* states. The GW direct band gaps of $SrSnO_3$ at high symmetry points are higher more than 3 eV (except R-R gap) in comparison to those values calculated in the GGA approach (Table 1).

The chemical compositions of $BaSnO_3$ and $SrSnO_3$ are similar. Therefore, *p* orbital character prevails in formation of the top of the valence band for those crystals. The Ba *p* states significantly contribute to the top of the valence band and form the bottom of the conduction band in $BaSnO_3$. Whereas the Sr *s, p, d* states create the lower part of the conduction band in $SrSnO_3$ crystal.

Recently, the band structure of (Ba,Sr)SnO_3 have been calculated using mBJ potential [18]. The obtained band gaps Γ-M are 2.49 eV and 3.12 eV in $BaSnO_3$ and $SrSnO_3$, respectively. While in other theoretical investigations the indirect gaps Γ-R have been found for (Ba,Sr)SnO_3 crystals [17, 35-37]. However, as can be seen, the indirect band gaps in (Ba,Sr)SnO_3, found within the GW method, are better compared with measured values than those obtained by other approaches.

The band gap value of 3.05 eV was obtained for crystal $BaSnO_3$ by means of the GW method with the plasmon pole model dielectric function [22]. This result is well compared with our GW calculation of the electronic structure of $BaSnO_3$ based on the contour defor-

mation method [27]. In previous works [23, 34] we have carried out the band structure calculations of cubic perovskites $RbMF_3$ (M = Be, Mg, Ca, Sr, Ba) as well as alkali metal chalcogenides using the contour deformation technique. All the obtained band gaps have revealed a good agreement with the experimental data.

4. CONCLUSIONS

First, we evaluated the electronic band energies of cubic perovskites $(Ba,Sr)SnO_3$ within the GGA approach. The corresponding band gaps were underestimated by more than 70 percent compared to experimental data. We looked for more accurate values of the electron energy using the Green's function, built on the basis of eigenstates, which were already calculated in the GGA approach. The indirect gaps of $(Ba,Sr)SnO_3$, obtained in the first order of perturbation theory (the GW approach) are close to the experimental values. The GW corrections led to a proper widening of indirect and direct band gaps, so the contour deformation method is suitable for cubic $(Ba,Sr)SnO_3$. The energy corrections obtained from the GW approximation for the valence band states are small. The differences between band gaps $\Delta = E_{GW} - E_{GGA}$ show a significant dispersion in the momentum space, and therefore the scissor operator, needed for calculation of optical constants, should be selected from the interval between minimal and maximal values of Δ. The GW method based on GGA eigenstates is applicable for the description of alkaline earth metal stannates like $BaSnO_3$ and $SrSnO_3$.

Структура електронних енергетичних зон перовскитів $BaSnO_3$ та $SrSnO_3$, обчислена за методами GGA та GW

С.В. Сиротюк, І.Є. Лопатинський, В.М. Швед

Національний університет "Львівська політехніка", вул. С. Бандери, 12, 79013 Львів, Україна

Метод функції Гріна, реалізований у першому порядку теорії збурення (GW), був застосований для точного опису електронної структури перовскітів кубічних (Ba, Sr) SnO_3. Спочатку електронна структура $(Ba,Sr)SnO_3$ була розрахована в рамках узагальненого градієнтного наближення (GGA). Далі для отримання точніших міжзонних щілин були розраховані квазічастинкові поправки до власних енергій. Електронні структури, отримані за допомогою наближень GGA та GW, детально порівнюються між собою. Застосування квазічастинкових поправок до власних енергій привело до значного розширення міжзонних щілин і гарного зіставлення з експериментальними даними. Поправки до зонних енергій, отримані за методом GW для обох кристалів у точках першої зони Бріллюена, досить різні. Отже, використання ножиць (scissor operator) може приводити до похибок в розрахунках оптичних констант.

Ключові слова: Перовскити, Електронна структура, Функція Гріна, Метод GW, Квазічастинки.

REFERENCES

1. L. Zhu, Z. Shao, J. Ye, X. Zhang, X. Pan, S. Dai, *Chem. Commun.* **52**, 970 (2016).
2. S. Ismail-Beigi, F.J. Walker, S.W. Cheong, K.M. Rabe, C.H. Ahn, *APL Mater.* **3**, 062510 (2015).
3. N. Sharma, K.M. Shaju, G.V. Subba Rao, B.V.R. Chowdari, *J. Power Sources* **139**, 250 (2005).
4. A. Marikutsa, M. Rumyantseva, A. Baranchikov, A. Gaskov, *Materials* **8**, 6437 (2015).
5. Y.P. Yuan, J. Lv, X.J. Jiang, Z.S. Li, T. Yu, Z.G. Zou, J.H. Ye, *Appl. Phys. Lett.* **91**, 094107 (2007).
6. W.F. Zhang, J.W. Tang, J.H. Ye, *Chem. Phys. Lett.* **418,** 174 (2006).
7. H.J. Kim, U. Kim, H.M. Kim, T.H. Kim, H.S. Mun, B. Jeon, K.T. Hong, W. Lee, C. Ju, K.H. Kim, K. Char, *Appl. Phys. Express* **5**, 061102 (2012).
8. E. Baba, D. Kan, Y. Yamada, M. Haruta, H. Kurata, Y. Kanemitsu, Y. Shimakawa, *J. Phys. D Appl. Phys.* **48**, 455106 (2015).
9. K. van Benthem, C. Elsässer, R.H. French, *J. Appl. Phys.* **90**, 6156 (2001).
10. S.A. Chambers, T.C. Kaspar, A. Prakash, G. Haugstad, B. Jalan, *Appl. Phys. Lett.* **108**, 152104 (2016).
11. S. Yu, D. Yoon, J. Son, *Appl. Phys. Lett.* **108**, 262101 (2016).
12. J. Shiogai, K. Nishihara, K. Sato, A. Tsukazaki, *AIP Advances* **6**, 065305 (2016).
13. H. Mizoguchi, H.W. Eng, P.M. Woodward, *Inorg. Chem.* **43**, 1667 (2004).
14. G. Larramona, C. Gutierrez, I. Pereira, M.R. Nunes, F.M.A. Dacosta, *J. Chem. Soc. Faraday Trans.* **85**, 907 (1989).
15. Q. Liu, B. Li, J. Liu, H. Li, Z. Liu, K. Dai, G. Zhu, P. Zhang, F. Chen, J. Dai, *EPL* **98**, 47010 (2012).
16. Y. Li, L. Zhang, Y. Ma, D.J. Singh, *APL Materials* **3**, 011102 (2015).
17. S. Li-Wei, D. Yi-Feng, Y. Xian-Qing, Q. Li-Xia, *Chin. Phys. Lett.* **27**, 096201 (2010).
18. M.B. Saddique, M. Rashid, A. Afzal, S.M. Ramay, F. Aziz, A. Mahmood, *Curr. Appl. Phys.***17**, 1079 (2017).
19. K.P. Ong, X. Fan, A. Subedi, M.B. Sullivan, D.J. Singh, *APL Materials* **3**, 062505 (2015).
20. S. Lee, H. Wang, P. Gopal, J. Shin, H.M. Iftekhar Jaim, X. Zhang, S.-Y. Jeong, D. Usanmaz, S. Curtarolo, M. Fornari, M. Buongiorno Nardelli, I. Takeuchi, *Chem. Mater.* **29**, 9378 (2017).
21. F. Aryasetiawan, O. Gunnarsson, *Rep. Prog. Phys.* **61**, 273 (1998).
22. H. Li, I.E. Castelli, K.S. Thygesen, K.W. Jacobsen, *Phys. Rev. B* **91**, 04520 (2015).
23. S.V. Syrotyuk, V.M. Shved, *Eur. Phys. J. B* **88**, 229 (2015).
24. M. Torrent, F. Jollet, F. Bottin, G. Zerah, X. Gonze, *Comp. Mater. Sci.* **42**, 337 (2008).
25. B. Arnaud, M. Alouani, *Phys. Rev. B* **62**, 4464 (2000).
26. M. Shishkin, G. Kresse, *Phys. Rev. B* **74**, 035101 (2006).
27. X. Gonze, F. Jollet, F.A. Araujo, D. Adams, B. Amadon, T. Applencourt, C. Audouze, J.-M. Beuken, J. Bieder, A. Bokhanchuk, E. Bousquet, F. Bruneval, D. Caliste, M. Côté, F. Dahm, F. Da Pieve, M. Delaveau, M.

Di Gennaro, B. Dorado, C. Espejo, G. Geneste, L. Genovese, A. Gerossier, M. Giantomassi, Y. Gillet, D. R. Hamann, L. He, G. Jomard, J. L. Janssen, S. Le Roux, A. Levitt, A. Lherbier, F. Liu, I. Lukačević, A. Martin, C. Martins, M.J.T. Oliveira, S. Poncé, Y. Pouillon, T. Rangel, G.-M. Rignanese, A.H. Romero, B. Rousseau, O. Rubel, A.A. Shukri, M. Stankovski, M. Torrent, M.J. Van Setten, B. Van Troeye, M.J. Verstraete, D. Waroquiers, J. Wiktor, B. Xu, A. Zhou, J.W. Zwanziger, *Comput. Phys. Commun.* **205**, 106 (2016).
28. H.J. Monkhorst, J.D. Pack, *Phys. Rev. B* **13**, 5188 (1976).
29. A.R. Tackett, N.A.W. Holzwarth, G.E. Matthews, *Comput. Phys. Commun.* **135**, 348 (2001).
30. S. Faleev, M. van Schilfgaarde, T. Kotani, *PRL* **93**, 126406 (2004).
31. T.H. Fischer, J. Almlof, *J. Phys. Chem.* **96**, 9768 (1992).
32. H.D. Megaw, *P. Phys. Soc. Lon.* **58**, 133 (1946).
33. A. Prakash, P. Xu, A. Faghaninia, S. Shukla, J.W. 3rd Ager, C.S. Lo, B. Jalan, *Nat. Commun.* **8**, 15167 (2017).
34. S.V. Syrotyuk, V.M. Shved, *Condens. Matter Phys.* **18**, 33702 (2015).
35. B. Ghebouli, M.A. Ghebouli, M. Fatmi, S. Boucetta, M. Reffas, *Solid State Commun.* **149,** 2244 (2009).
36. T.N. Stanislavchuk, A.A. Sirenko, A.P. Litvinchuk, X. Luo, S.-W. Cheong, *J. Appl. Phys.* **112**, 044108 (2012).
37. J. Li, Z. Ma, R. Sa, K. Wu, *RSC Adv.* **7**, 32703 (2017).